scientific reports

Check for updates

OPEN

Numerical analysis of thermal conductive hybrid nanofluid flow over the surface of a wavy spinning disk

Ali Ahmadian[1], Muhammad Bilal[2], Muhammad Altaf Khan[3,4]✉ & Muhammad Imran Asjad[5]

A three dimensional (3D) numerical solution of unsteady, Ag-MgO hybrid nanoliquid flow with heat and mass transmission caused by upward/downward moving of wavy spinning disk has been scrutinized. The magnetic field has been also considered. The hybrid nanoliquid has been synthesized in the presence of Ag-MgO nanoparticles. The purpose of the study is to improve the rate of thermal energy transmission for several industrial purposes. The wavy rotating surface increases the heat transmission rate up to 15%, comparatively to the flat surface. The subsequent arrangement of modeled equations is diminished into dimensionless differential equation. The obtained system of equations is further analytically expounded via Homotopy analysis method HAM and the numerical Parametric continuation method (PCM) method has been used for the comparison of the outcomes. The results are graphically presented and discussed. It has been presumed that the geometry of spinning disk positively affects the velocity and thermal energy transmission. The addition of hybrid nanoparticles (silver and magnesium-oxide) significantly improved thermal property of carrier fluid. It uses is more efficacious to overcome low energy transmission. Such as, it provides improvement in thermal performance of carrier fluid, which play important role in power generation, hyperthermia, micro fabrication, air conditioning and metallurgical field.

Abbreviations

S	Control upward/downward motion of the disk
T	Fluid temperature (K)
γ	Disk temperature parameter
T_∞	Temperature away from the surface
Ha	Hartmann number
(r, θ, z)	Cylindrical coordinate
η	Similarity variable
ν	Kinematic viscosity $\left(\mathrm{m^2\ s^{-1}}\right)$
Pr	Prandtl number
Θ	Dimensionless temperature
σ	Thermal conductivity
$\phi_1 = \phi_{Ag}$	Volume fraction of silver
k_{hnf}	Thermal conductivity
ρ_{s1}	Silver specific heat capacity
ρ_{hnf}	Hybrid Nanofluid density
Ag	Silver
PCM	Parametric continuation method
u, v, w	Velocity component
T_w	Temperature of the Surface
β	Permeability parameter

[1]Institute of IR 4.0, The National University of Malaysia (UKM), 43600 Bangi, Selangor, Malaysia. [2]Department of Mathematics, City University of Science and Information Technology, Peshawar, Pakistan. [3]Informetrics Research Group, Ton Duc Thang University, Ho Chi Minh City, Vietnam. [4]Faculty of Mathematics and Statistics, Ton Duc Thang University, Ho Chi Minh City, Vietnam. [5]Department of Mathematics, University of Management and Technology Lahore, Lahore, Pakistan. ✉email: muhammad.altaf.khan@tdtu.edu.vn

p(Pa)	Pressure
θ	Direction of the magnetic field
f, g, h	Dimensional velocity
Z	Vertical distance
μ	Dynamic viscosity $\left(\mathrm{k\,g\ m^{-1}s^{-1}}\right)$
μ_{hnf}	Dynamic viscosity of nanofluid
ω	Velocity (vertical) of disk $\left(\mathrm{r\ s^{-1}}\right)$
Ω	Velocity (angular) of disk $\left(\mathrm{r\ s^{-1}}\right)$
$\phi_2 = \phi_{MgO}$	Magnesium oxide volume fraction
α	Thermal diffusivity $\left(\mathrm{m^2\ s^{-1}}\right)$
ρ_{s2}	Magnesium oxide specific heat capacity
ν_{hnf}	Nanofluid kinematic viscosity
MgO	Magnesium oxide
HAM	Homotopy analysis method

The transmission of heat with the fluid flow has been a great area of research due to its wide application in the field of electronic devices and heat exchanger[1]. To escalate the heat transport and improve the flow pattern the extended surface is highly effective configuration. The heat transfer characteristic and fluid flow of the Sinusoidal-Corrugated channels are numerically investigated by Khoshvaght-Aliabadi[2]. The parameter effect including length of wave and amplitude, channel height and length, volume fraction of nanoparticle and Reynolds number were analyzed. Rashidi et al.[3] tackled flow field and the heat transmission through a wavy channel. The uniform suction upshots deploy on the flow due to spinning disk is investigated by Stuart[4]. In early studies the heat transfer on rotating disk was examined by[5]. As flow started from rest, the steady motion of flow was obtained numerically by[6]. Kuiken[7] clarified the blowing effect induced by porous rotating disk. Turkyilmazoglu[8] reported the effect of stretching disk surface. Tabassum and Mustafa[9] considered non-Newtonian Reiner-Rivlin fluid about rotating disk. Asifa et al.[10] explores the behavior of an incompressible hybrid nanoliquid flow over an impermeable infinite spinning disk. Shuaib et al.[11] has highlighted the 3D an incompressible fluid flow with heat transport over stretchable revolving disk.

Conventional fluid Such as, ethylene glycol, oil and water are play a conspicuous role in heat transfer, for example, in chemical processes, in cooling or heating processes, in power generation and in some other small electronics mechanism. But comparatively, the thermal energy transmission rate of these liquids very low and cannot accomplished the need of high rates of heat exchange. To overcome this deficiency, the nanometer-sized particles (1–100 nm), termed as nanoparticle is added to common fluid to enhance its thermal conductivity. The word 'nanofluid' was first used by Choi[12], which show high thermal conductivity, better rheological properties and stability as compared to fluid having micronized particles. The researcher used a variety of technique to prepare different types of nanoparticle to calculate the thermo physical properties[13]. Due to possessing the ability of dispersing and oil wetting nanoparticle is used to clean the surface in engineering purposes. It provides improvement in thermal performance, which play important role in power generation, hyperthermia, micro fabrication, air conditioning and metallurgical field. Magnesium oxide MgO compound consists of Mg^{2+} and O^{2-} ions, together bonded by strong ionic bond which can be synthesized by the calcination of magnesium hydroxide $Mg\ (OH)^2$ and $MgCO^3$ (magnesium carbonate) at 700–1500 °C. It is mostly efficacious for refractory and electrical applications. Similarly, the antibacterial upshots of silver Ag nano-size particles have been used to manage the bacterial growth in a several applications, such as dental work, burns and wound treatment, surgery applications and biomedical apparatus. The silver-based compounds and silver ions are highly toxic to microorganisms. Hussanan et al.[14] examined the Oxide nanoparticles for the up gradation of energy in engine nanofluids, kerosene oil and water. Acharya and Mabood[15] have studied the hydrothermal characteristics of both common nanoliquid and hybrid nanoliquid flow over a permeable slippery bent surface using Runge Kutta fourth order Method RK-4. The heat transmission and flow pattern in presence of solar radiation of hybrid nanoliquid for several solar thermal apparatus is revealed by[16]. They considered Copper-Alumina nano-ingredients with the base fluid. To refine the heat transmission in an inclined cavity Motlagh and Soltanpour[17] used Al_2O_3 Aluminum Oxide. The size, type, preparation method, dispersibility of nanoparticles, compatibility and purity of base fluid and nanoparticle greatly affects the thermal properties of nanofluids. The most common used nanoparticles in base fluids are metal oxides Fe_2O_3, MgO, Al_2O_3, TiO_3, CuO, metal nitride AIN, Carbon nanotubes and metal like (Au, Ag, Ni, Cu) etc. Acharya et al.[18] scrutinized the hybrid nanoliquid flow with the Hall current characteristics under the magnetic and thermal radiation effects over a spinning disk. They considered an innovative class of nanoliquid consists of Titanium Dioxide ($TiO2$) and Copper (Cu) nanoparticles. The magnetic effect on the flow with SWCNTs and MWCNTs over a moving/static wedge in a permeable channel was calculated by Akber et al.[19]. Some relevant literature related to the present work is present in[20,21].

The perturbation methods are mostly used for the solution of non-linear problems, to find its approximate solutions. However, it depends on small/large parameters, due to which it cannot be widely used. For the non-linear problems an analytic tool (HAM) was introduced by Liao[22], which is based on topology concept[23]. The HAM (Homotopy Analysis Method) has many advantages such as, it provides us more convenient way than any other analytic method to control the series solution convergence and even it can be applied to those problems, which do not have any small/large parameters[24]. This technique has been already used for several non-linear problems to obtain its analytic solutions[25]. Muhammad et al.[26] studied the entropy generation, thermal and momentum proclamation on boundary layer flow over a linear surface using HAM technique. The MHD (magnetohydrodynamic) flow of nanoliquid over a spinning disk consist of silver Ag particles, with variable thickness using HAM procedure is scrutinized by Doh et al.[27]. They presumed that the all the velocities of rotating surface rises with

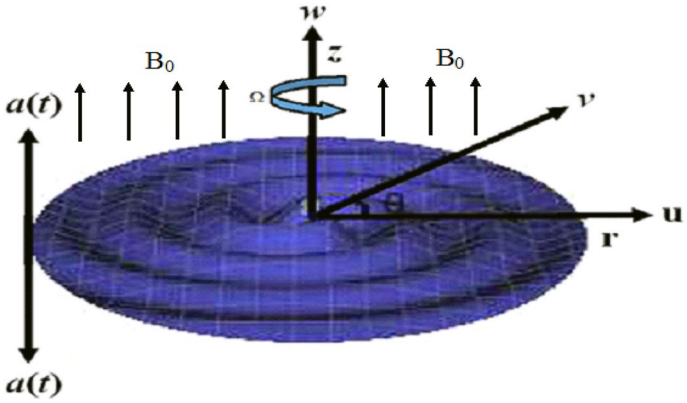

Figure 1. Wavy disk.

	$\rho(kg/m^3)$	$C_p(j/kgK)$	$k(W/mK)$	$\beta \times 10^5(K^{-1})$
Pure water	997.1	4179	0.613	21
Magnesium oxide	3560	955	45	1.80
Silver	10,500	235	429	1.89

Table 1. Numerical properties of the water and hybrid nanofluid [29].

positive increment in disk thickness. Asifa et al.[10] highlighted the fine point of CNTs hybrid nanoliquid flow over revolving surface using HAM technique. They noticed that, the growing credit of disk rotation significantly accelerate the heat transmission rate and fluid velocity. The steady magnetic flow of nanoliquid via a porous surface with slip conditions and viscous dissipation by employing HAM technique is discussed by Alreshidi et al.[28].

The ambition of consideration is to extend the idea of Ref.[29] and to investigate the effect of two different nanoparticle Silver Ag and magnesium oxide MgO/Water hybrid nanoliquids over a wavy rotating disk, with upward/downward movement. To improve the thermal conductivity of the fluid flow, this study is taken under consideration. The modeled equations are solved analytically via HAM and for validation and comparison purpose of the outcomes, the Parametric continuation method (PCM) has been implemented. Both results manifest best consensus with each other (Fig. 1).

Mathematical formulation

This section will explain the physical interpretation of the problem, thermophysical properties and equation of motion.

Physical description of the problem. Let us consider a three-dimensional flow of Silver magnesium oxide hybrid Ag-MgO/Water nanoliquid over upward/downward moving wavy rotating disk. At time t, the disk has a vertical velocity $\omega = a(t)$ and is at a vertical distance $Z = a(t)$. The disk was $a(0) = h$ at $t = 0$. The rotating disk has angular velocity $\Omega(t)$ about $z-$ axis, the buoyancy effects are negligible and it has been assumed that the nanoparticle are distributed consistent and be in equilibrium state. The uniform magnetic field of constant magnitude $\vec{B} = (B_r\vec{e}_r + B_\theta\vec{e}_\theta)$ and $B = \sqrt{B_r^2 + B_\theta^2}$ is applied respectively, where $\vec{e}_r$ and $\vec{e}_\theta$ are unit vectors.

Thermophysical properties of nanoliquid. The specific heat capacity and the density of the hybrid nanoliquid can be expounded are as follow[29]:

$$\left(\rho C_p\right)_{hnf} = \left\{(1-\varphi_2)\left[(1-\varphi_1)\left(\rho C_p\right)_f + \varphi_1\left(\rho C_p\right)_{s1}\right]\right\} + \varphi_2\left(\rho C_p\right)_{s2}, \tag{1}$$

$$\rho_{hnf} = \left\{(1-\varphi_2)\left[(1-\varphi_1)_{\rho_f} + \varphi_1\rho_{s1}\right]\right\} + \varphi_2\rho_{s2}, \tag{2}$$

where ρ_{s1}, ρ_{s2} are the density, $\left(C_p\right)_{s1}, \left(C_p\right)_{s2}$ are specific heat capacity and φ_1, φ_2 are the volume fraction of the silver and magnesium oxide nanoliquid respectively, which are mentioned in Table 1.

The viscosity μ_{hnf} of nanofluid is calculated by curve fitting on real experimental data[29].

$$\mu_{hnf} = \left(1 + 2.5\varphi_1 + 6.2\varphi_2^2\right)\mu_f. \tag{3}$$

Here, the Prandtl number and the thermal conductivity of nanoliquid are defined as[29]:

$$\Pr_{hnf} = \frac{(\mu C_p)_{hnf}}{k_{hnf}},\ k_{hnf} = -\frac{q_w}{\partial\theta/\partial y}. \tag{4}$$

Equation of motion. The governing equation for unsteady, incompressible, MHD forced convective flow is defined as[29,30]:

$$\frac{\partial u}{\partial r} + \frac{\partial w}{\partial z} + \frac{u}{r} = 0, \tag{5}$$

$$\rho_{hnf}\left(\frac{\partial u}{\partial t} + u\frac{\partial u}{\partial r} + w\frac{\partial u}{\partial z} - \frac{v^2}{r}\right) = -\frac{\partial p}{\partial r} + \mu_{hnf}\left(\frac{\partial^2 u}{\partial r^2} + \frac{\partial^2 u}{\partial z^2} + \frac{1}{r}\frac{\partial u}{\partial r} - \frac{u}{r^2}\right) + F_r, \tag{6}$$

$$\rho_{hnf}\left(\frac{\partial v}{\partial t} + u\frac{\partial v}{\partial r} + w\frac{\partial v}{\partial z} - \frac{uv}{r}\right) = \mu_{hnf}\left(\frac{\partial^2 v}{\partial r^2} + \frac{\partial^2 v}{\partial z^2} + \frac{1}{r}\frac{\partial v}{\partial r} - \frac{v}{r^2}\right), \tag{7}$$

$$\rho_{hnf}\left(\frac{\partial w}{\partial t} + u\frac{\partial w}{\partial r} + w\frac{\partial w}{\partial z}\right) = -\frac{\partial p}{\partial r} + \mu_{hnf}\left(\frac{\partial^2 w}{\partial r^2} + \frac{\partial^2 w}{\partial z^2} + \frac{1}{r}\frac{\partial w}{\partial r}\right) + F_\theta, \tag{8}$$

$$\left(\frac{\partial T}{\partial t} + u\frac{\partial T}{\partial r} + w\frac{\partial T}{\partial z}\right) = \frac{k}{(\rho C_p)_{hnf}}\left(\frac{\partial^2 T}{\partial r^2} + \frac{1}{r}\frac{\partial T}{\partial r} + \frac{\partial^2 T}{\partial z^2}\right). \tag{9}$$

Here body forces F_r along x and F_θ along z direction respectively. It can be expressed as[29]:

$$F_r = \frac{Ha^2\mu_{hnf}}{R^2}\left(v\sin\theta\cos\theta - u\sin^2\theta\right), \tag{10}$$

$$F_\theta = \frac{Ha^2\mu_{hnf}}{R^2}\left(u\sin\theta\cos\theta - v\sin^2\theta\right). \tag{11}$$

Here $u,\ v,\ w$ is the velocity component of the fluid, while Ha is $LB_0\sqrt{\frac{\sigma}{\mu}}$, in which B_0 is the magnitude and θ is the direction of magnetic field.

Boundary condition. The initial and boundary condition for wavy spinning disk are:

$$u = 0,\ v = r\Omega_0(t),\ w = w_0(t),\ T = T_0,\ \text{at } z = 0$$

$$u \to 0,\ v \to 0,\ w \to 0,\ T \to T_\infty,\ \text{at } z \to \infty. \tag{12}$$

Karman's approach. In order to transform the Eqs. (5–9) and (12) to the system of ODEs, we use the following transformation, we follow[30].

$$u = \frac{rv}{a^2(t)}f(\eta),\ v = \frac{rv}{a^2(t)}g(\eta),\ w = \frac{v}{a(t)}h(\eta),\ p = \frac{pv^2}{a^2(t)}p(\eta),$$

$$T = T_\infty + \Delta T_\infty,\ \eta = \frac{Z}{a(t)} - 1,\ \eta_Z = \frac{1}{a(t)},\ \eta_t = \frac{-a(t)}{a(t)}(\eta + 1). \tag{13}$$

The following system of ordinary differential equation is formed by using Eq. (13) in Eqs. (5–9):

$$f'' = \frac{\rho_{hnf}}{\mu_{hnf}}\left(hf' + f^2 - g^2 - S\frac{(\eta+1)f'}{2} + f\right) + A\omega\left(g\sin\theta\cos\theta - f\sin^2\theta\right), \tag{14}$$

$$g'' = \frac{\rho_{hnf}}{\mu_{hnf}}\left(hg' + 2fg - S\left(\frac{(\eta+1)g'}{2} - g\right)\right), \tag{15}$$

$$h'' = \frac{\rho_{hnf}}{\mu_{hnf}}\left(hh' - S\frac{(\eta+1)h'}{2} + h'\right) - A\omega\left(f\sin\theta\cos\theta - g\sin^2\theta\right), \tag{16}$$

$$\theta'' = \rho_{hnf}\left(h\theta' - S\left(\frac{(\eta+1)\theta'}{2} + \gamma\theta\right)\right). \tag{17}$$

The diminished conditions are:

$$f(0) = 0,\ h(0) = \beta\frac{S}{2},\ g(0) = \omega,\ \theta(0) = 1,\ \text{at}\ \eta = 0,$$

$$f(\eta) \to 0,\ g(\eta) \to 0,\ h(\eta) \to 0,\ \theta(\eta) \to 0,\ \text{as}\ \eta = \infty. \tag{18}$$

Since the physical constraint S controlling the up/down movement of the disk (or the contraction/expansion of the disk) is defined as[30]:

$$S = 2\frac{a^*(t)a(t)}{\nu}, \tag{19}$$

Sign ω nominate the constant rotation of wavy disk[30]:

$$\omega = 2\frac{a^2(t)\Omega(t)}{\nu}. \tag{20}$$

And disk temperature parameter, which express temperature distribution:

$$\gamma = \frac{1}{2}\frac{a(t)T}{a^*(t)\Delta T}. \tag{21}$$

The non-dimensional form of Nusselt number and skin friction are expressed as:

$$Nu = \frac{rq_w}{k_f(T_w - T_\infty)}\ \text{ and }\ C_f = \frac{\sqrt{\tau_{wr}^2 - \tau_{w\phi}^2}}{\rho_f(\Omega\, r)^2}. \tag{22}$$

where, $\tau_{w\phi}$ and $\tau_{w\,r}$ stand for transverse and radial stress respectively.

Problem solution

The analytical approach HAM, which was presented by Liao[22–24] has been used for the solution of nonlinear modeled differential equations. For strong convergence, BVP 2.0 package has been implementing to show sum of square residual error.

The linear operators π_f,π_g,π_h and π_Θ are presented as,

$$\pi_f = \frac{\partial^2 f}{\partial\eta^2},\ \ \pi_g = \frac{\partial^2 g}{\partial\eta^2},\ \ \pi_h = \frac{\partial^2 h}{\partial\eta^2},\ \ \pi_\theta = \frac{\partial^2\theta}{\partial\eta^2}. \tag{17}$$

The expand form of π_f,π_g,π_h and π_Θ are ,

$$\pi_f(\chi_1 + \chi_2\eta) = 0,\ \ \pi_g(\chi_3 + \chi_4\eta) = 0,\ \ \pi_h(\chi_5 + \chi_5\eta) = 0\ \text{ and }\ \pi_\Theta(\chi_4 + \chi_5\xi) = 0. \tag{22}$$

Taylor's series expansion form is used

$$f(\eta;\rho) = f_0(\eta) + \sum_{x=1}^{\infty} f_x(\eta)\rho^x, \tag{23}$$

$$g(\eta;\rho) = g_0(\eta) + \sum_{x=1}^{\infty} g_x(\eta)\rho^x, \tag{24}$$

$$h(\eta;\rho) = h_0(\eta) + \sum_{x=1}^{\infty} h_x(\eta)\rho^x, \tag{25}$$

$$\theta(\xi;\rho) = f_0(\xi) + \sum_{x=1}^{\infty} \theta_x(\xi)\rho^x, \tag{26}$$

Now

$$\begin{aligned} &f_x(\eta) = \frac{1}{x}\frac{df(\eta;\rho)}{d\eta}|_{\rho=0},\quad g_x(\eta) = \frac{1}{x}\frac{dg(\eta;\rho)}{d\eta}|_{\rho=0},\ h_x(\eta) = \frac{1}{x}\frac{dh(\eta;\rho)}{d\eta}|_{\rho=0}\,,\\ &\theta_x(\eta) = \frac{1}{x}\frac{d\theta(\eta;\rho)}{d\eta}|_{\rho=0}. \end{aligned} \tag{27}$$

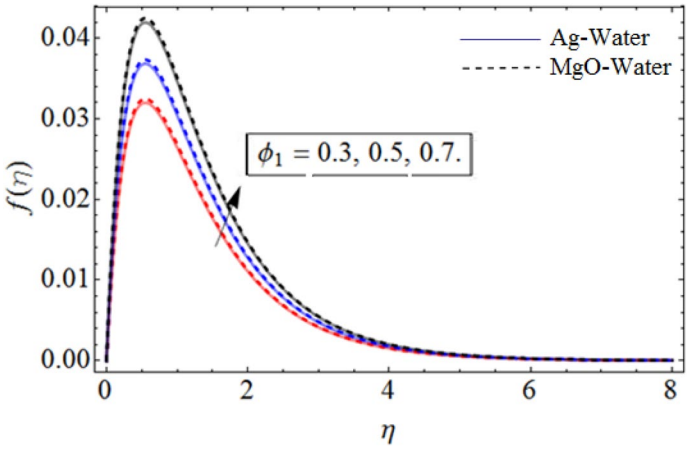

Figure 2. ϕ_1 out-turn versus axial velocity $f(\eta)$. When Pr $= 6.7, \beta = 0.7, \phi_2 = 0.9, S = 2.2, \omega = 1.0$.

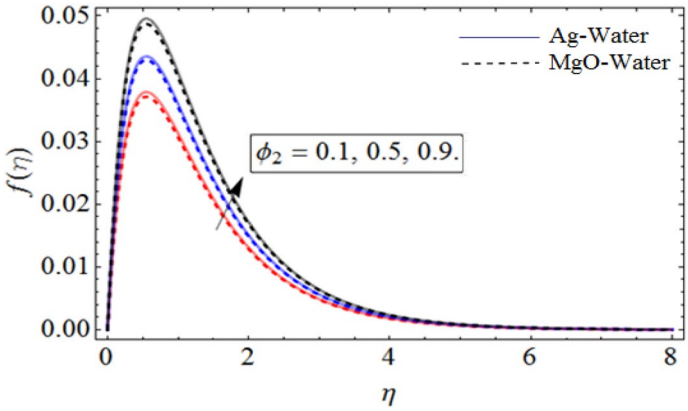

Figure 3. ϕ_2 out-turn versus the axial velocity $f(\eta)$. When Pr $= 6.7,\ \beta = 0.7, \phi_1 = 0.7, S = 2.2, \omega = 1.0$.

The system of equation can be written in the form of:

$$L_f\left[f_x(\eta) - N_x f_{x-1}(\eta)\right] = \pi_f R_x^f(\eta), \tag{28}$$

$$L_g\left[g_x(\eta) - N_x g_{x-1}(\eta)\right] = \pi_g R_x^g(\eta), \tag{29}$$

$$L_h[h_x(\eta) - N_x h_{x-1}(\eta)] = \pi_h R_x^h(\eta), \tag{30}$$

$$L_\theta[\theta_x(\eta) - N_x \theta_{x-1}(\eta)] = \pi_\theta R_x^\theta(\eta), \tag{31}$$

where $N_x = 0$ if $\rho \leq 1$ and if $\rho > 1$.

Result and discussion

The time dependent, 3D hybrid nanoliquid flow over a wavy rotating disk with upward/downward motion has been studied. The numerical results of the system of differential equations has been acquire through Parametric continuation method (PCM), while for comparison and validity of results and to get analytical output, HAM technique has been applied. The effect of physical parameter has been shown in Figs. 2, 3, 4, 5, 6, 7, 8, 9, 10 and 11. For comparative studies of PCM and HAM, Tables 2, 3 and Tables 4 are plotted.

Figure 1 displays the hybrid nanofluid flow over a wavy spinning disk under the magnetic effects. Figures 2 and 3 demonstrate the influence of volume fraction parameter ϕ_1 or ϕ_{Ag} and ϕ_2 or ϕ_{MgO} on axial velocity profile $f(\eta)$. It shows that, by increasing the number of silvers Ag and magnesium oxide nanoparticles, the axial velocity of fluid significantly improve. Figure 4 highlights the dominance of unsteadiness parameter S versus axial velocity $f(\eta)$**.** The rising credit of S declines the fluid velocity. Figure 5 depicts the out-turn of rotation parameter ω on the radial velocity $g(\eta)$. It can be presumed that, the increment in ω increases the kinematic energy of the

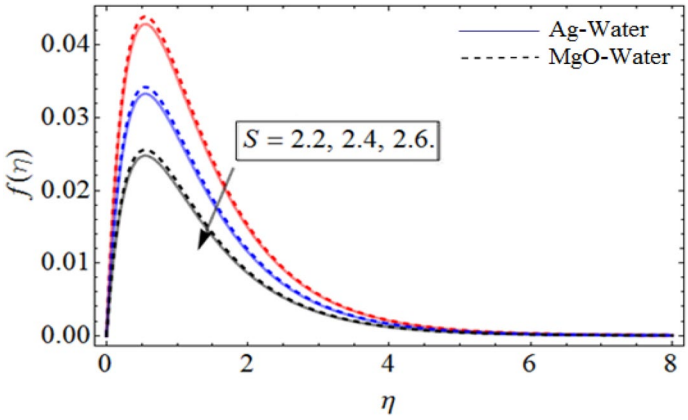

Figure 4. S out-turns versus the axial velocity $f(\eta)$. When $\mathrm{Pr} = 6.7, \beta = 0.7, \phi_1 = 0.7, \phi_2 = 0.9, \omega = 1.0$.

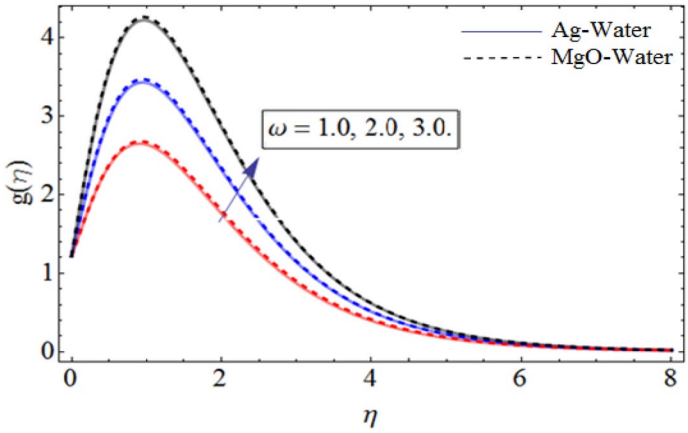

Figure 5. ω out-turn versus the radial velocity $g(\eta)$ When $\mathrm{Pr} = 6.7, \gamma = 0.3, \beta = 0.7, \phi_1 = 0.7, \phi_2 = 0.9$.

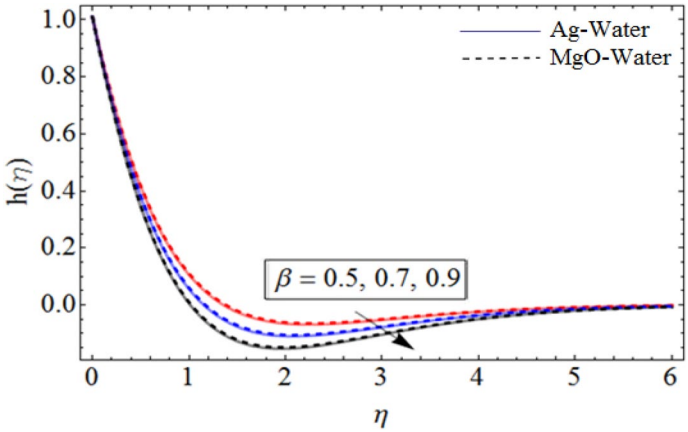

Figure 6. β out-turn versus the azimuthal velocity $h(\eta)$. When $\mathrm{Pr} = 6.7, \phi_1 = 0.7, \phi_2 = 0.9, S = 2.2, \omega = 1.0$.

fluid particles, consequently, the velocity accumulates, which generate some amount of heat. Eventually, the disk surface becomes heated, which also improve the fluid temperature $\theta(\eta)$.

Figures 6 and 7 show the upshot of β and controlling parameter S on the azimuthal velocity respectively. As S control the movement of the spinning disk, when we increases the values of S, the rate of upward/downward motion of the disk also increases. So, the inter-molecular forces between the fluid particles become week, and

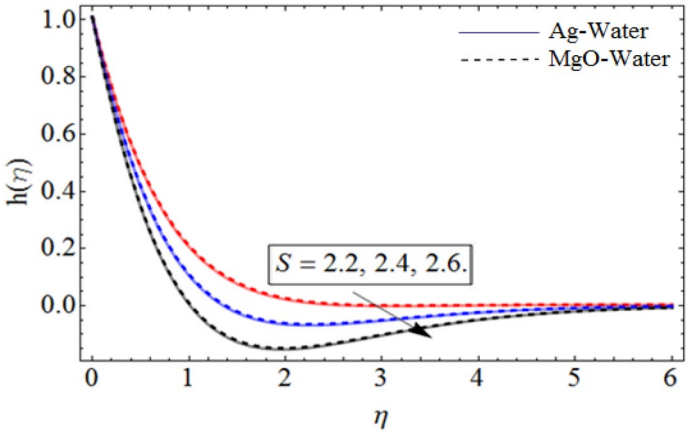

Figure 7. S out-turns versus the azimuthal velocity $h(\eta)$. When $\mathrm{Pr} = 6.7, \beta = 0.7, \phi_1 = 0.7, \phi_2 = 0.9, \omega = 1.0$.

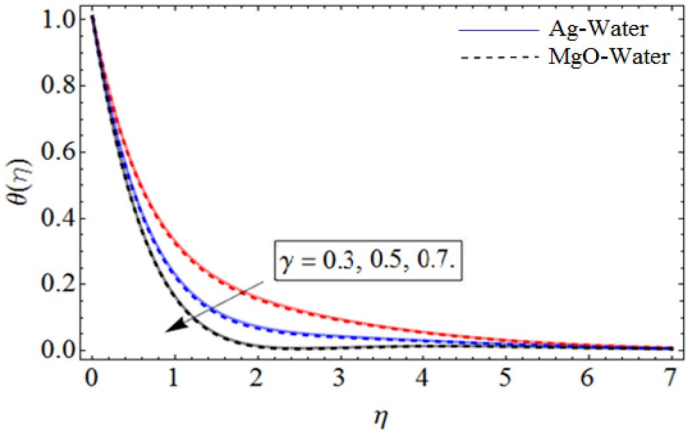

Figure 8. γ out-turn versus temperature profile $\theta(\eta)$. When $\mathrm{Pr} = 6.7, \beta = 0.7, \phi_1 = 0.7, \phi_2 = 0.9, \omega = 1.0$.

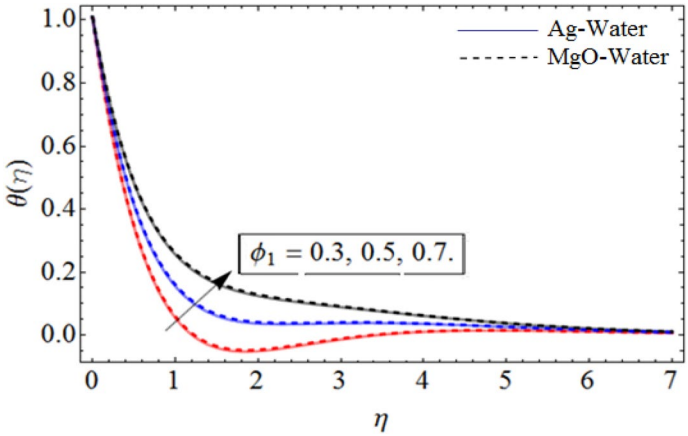

Figure 9. ϕ_1 out-turn versus the temperature profile $\theta(\eta)$. When $\mathrm{Pr} = 6.7, \beta = 0.7, \phi_2 = 0.9, S = 2.2, \omega = 1.0$.

during the upward motion of the disk the fluid molecule loses its energy, which causes the decline of temperature and azimuthal velocity as well.

Figure 8 depict the effects of γ on temperature. Parameter γ actually controls the upward and downward velocity of spinning disk. So, from Fig. 8, we can presume that the increasing values of γ will reduced the hybrid nanofluid temperature. Figures 9 and 10 illustrate the influence of ϕ_1 and ϕ_2 on temperature profile $\theta(\eta)$

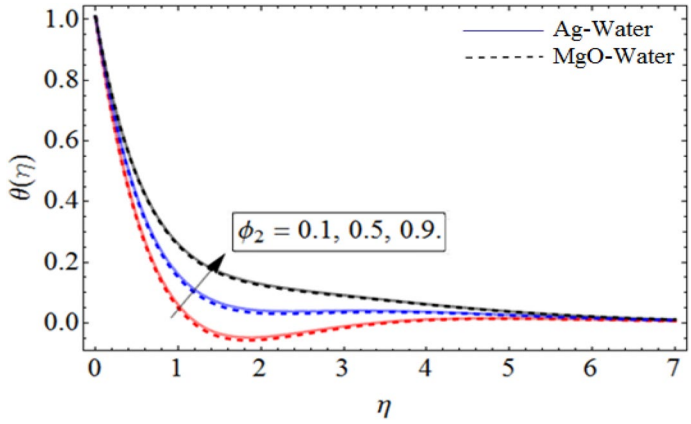

Figure 10. ϕ_2 out-turn versus the temperature $\theta(\eta)$. When $\mathrm{Pr} = 6.7, \beta = 0.7, \phi_1 = 0.7, S = 2.2, \omega = 1.0$.

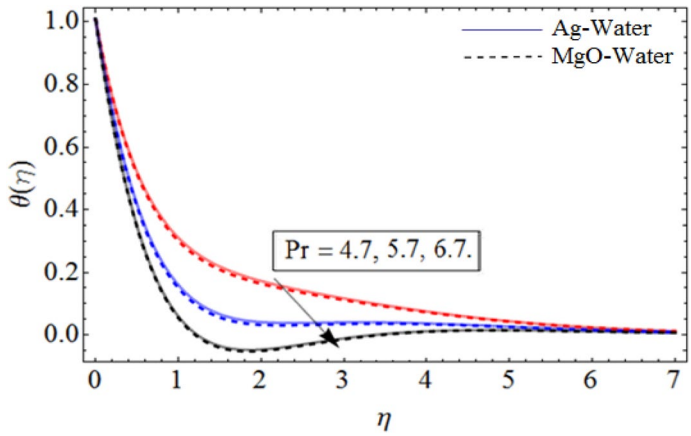

Figure 11. *Pr* out-turn versus the temperature $\theta(\eta)$. When $\beta = 0.7, \phi_1 = 0.7, \phi_2 = 0.9, S = 2.2, \omega = 1.0$.

	PCM (numerical results)			HAM (analytical results)		
η	$f(\eta)$	$g(\eta)$	$\theta(\eta)$	$f(\eta)$	$g(\eta)$	$\theta(\eta)$
0.0	0.0000	0.0000	1.0000	0.0000	0.0000	1.0000
0.5	0.0001	0.0010	0.2811	0.0001	0.0010	0.2821
1.0	0.0050	0.0147	0.0562	0.00051	0.01478	0.0562
1.5	−0.0381	−0.0761	0.0083	−0.0383	−0.0765	0.0087
2.0	−0.1369	−0.1903	0.0009	−0.1370	−0.1904	0.0009

Table 2. Numerical comparison of PCM method versus HAM for the physical parameters $S = 2.1, \mathrm{Pr} = 2.7, \gamma = 0.04, \phi_1 = 1.1, \phi_2 = 0.75, A = 1.2, W = 0.04$ and $B = 0.3$.

respectively. As the volume fraction of silver and magnesium *MgO* nanoparticles increase, the heat absorbing ability of fluid also increased, which result in enhancement of fluid temperature $\theta(\eta)$. Figure 9 shows the decreases of temperature versus increases in Prandtl number. $\mathrm{Pr}_{hnf} = \left(\mu C_p\right)_{hnf} / k_{hnf}$, physically less Prandtl fluid has higher thermal diffusivity. The thermal boundary layer thickness reduces with larger values of Prandtl number as a result in decrease of the temperature. Figures 12, 13, and 14 revealed the *h*-curves for axial velocity h_f, radial velocity h_g and temperature h_Θ fields respectively.

Table 2 illustrates the numerical comparison of PCM method against HAM approach for radial, azimuthal, and axial velocity. From Table 2, it can be observed that fractional model show fast converges than Runge Kutta order 4 method.

Table 3 shows comparative effect of volume fraction parameter ϕ on radial and tangential velocities $\left(f'(0), g'(0)\right)$ for different nanofluid, keeping the rest physical parameters are constant. From, Table 3 we can

η	Silver (Ag)		Magnesium oxide *MgO*	
	$f'(0)$	$g'(0)$	$f'(0)$	$g'(0)$
0.00	1.4725	1.6912	1.6323	1.7562
0.05	1.6134	1.7724	1.9735	1.8821
0.01	1.8642	1.9054	2.2012	1.9922
0.15	2.0500	2.1791	2.3700	1.3901
0.20	2.3531	2.4753	2.5531	2.6102

Table 3. It shows the comparative behavior of *Ag* and *MgO* on radial and tangential velocities $\left(f'(0),\ g'(0)\right)$ for volume fraction parameter.

η	Silver (Ag)		Magnesium oxide *MgO*	
	$h'(0)$	$\theta'(0)$	$h'(0)$	$\theta'(0)$
0.00	1.3724	1.7954	1.6513	1.7582
0.05	1.3921	1.5362	1.4835	1.8734
0.10	1.6139	1.3482	0.2012	1.8622
0.15	0.4612	1.8014	1.4910	2.4684
0.20	0.5917	1.7961	2.7893	2.6212

Table 4. The numerical output of skin fraction and Nusselt number $h'(0), \theta'(0)$.

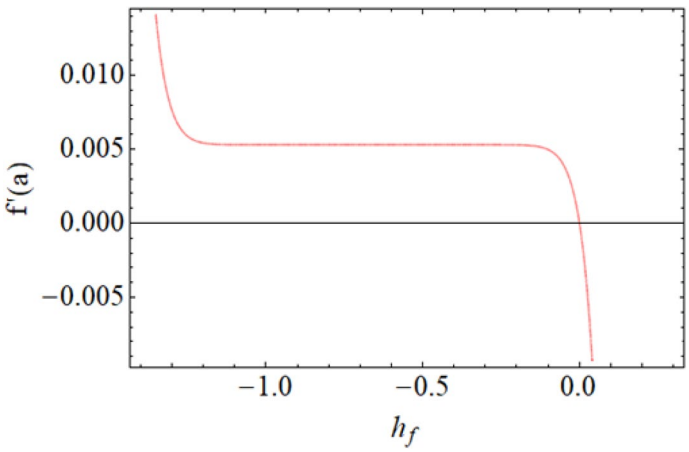

Figure 12. h_f When $\beta = 0.7, \phi_1 = 0.7, \phi_2 = 0.9, S = 2.2, \omega = 1.0$.

examine that, the radial and tangential velocity of *MgO* nanofluid are greater than the Silver Ag nanofluid, because the density of Silver nanoparticles are heavy than *MgO* nanoparticles. Therefore, the viscosity of Ag nanofluid is greater than *MgO* nanofluid. That's the reason that the radial and tangential velocity of *MgO* nanofluid is greater.

Table 4 shows the comparative effect of volume fraction parameter ϕ on skin fraction and Nusselt number $h'(0)$ and $\theta'(0)$ for different nanofluid respectively while the rest of physical parameters are constant. The sum and square of the total residual for the *Ag* and *MgO* are displayed in Tables 5 and 6. Table 7 displays the comparison of present work with the published literature.

Conclusion

In this work, the three-dimensional, unsteady *Ag-MgO*/water hybrid nanofluid flow, caused by upward/downward movement of a wavy rotating disk, under the magnetic field influence with mass and heat transport has been studied. The following observations have been made on the basis of above computation:

- The wavy rotating surface increases the heat transmission rate up to 15%, comparatively to flat surface[32].
- The rising credit of rotation parameter ω increases the kinematic energy of fluid, which result in the enhancement of velocity and temperature of hybrid nanoliquid.

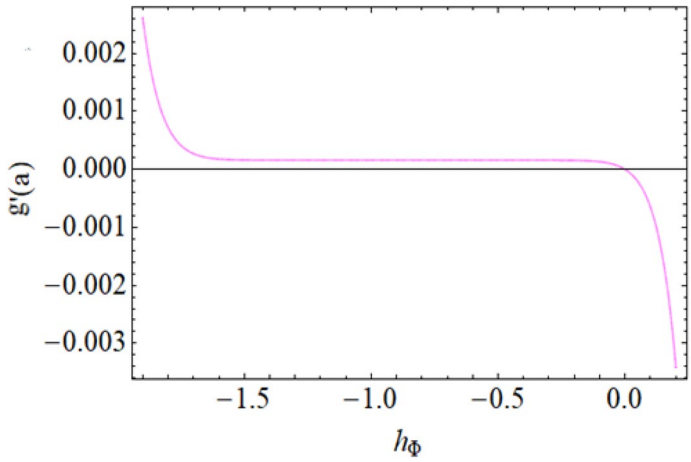

Figure 13. h_g When $\beta = 0.7, \phi_1 = 0.7, \phi_2 = 0.9, S = 2.2, \omega = 1.0$.

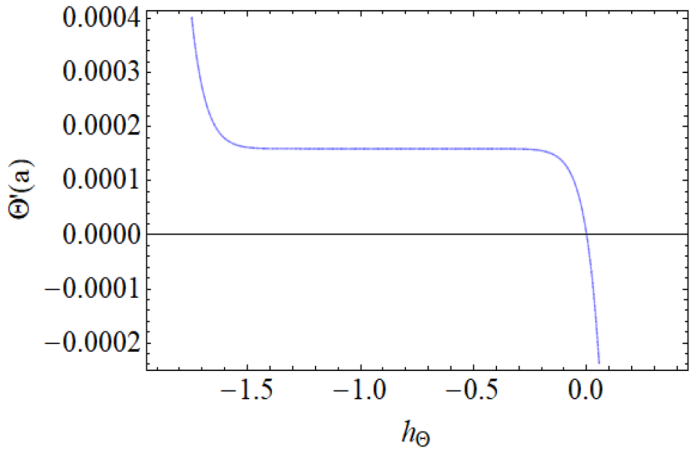

Figure 14. h_Θ When $\beta = 0.7, \phi_1 = 0.7, \phi_2 = 0.9, S = 2.2, \omega = 1.0$.

m	ε_m^f Ag	ε_m^g Ag	ε_m^h Ag	ε_m^θ Ag
3	5.15485×10^{-3}	4.87652×10^{-7}	5.57668×10^{-3}	4.24884×10^{-3}
6	3.53455×10^{-3}	3.94355×10^{-9}	5.1578×10^{-3}	2.3572×10^{-3}
9	1.48664×10^{-4}	7.41788×10^{-11}	4.14877×10^{-4}	3.54206×10^{-4}
12	6.21764×10^{-5}	2.85429×10^{-11}	3.1687×10^{-5}	4.2456×10^{-4}

Table 5. Total squares residual errors for silver Ag. When $\Pr = 6.3$, $\beta = 0.3$, $\phi_1 = 0.2$, $\phi_2 = 0.4$, $\omega = 0.75$.

m	ε_m^f MgO	ε_m^g MgO	ε_m^h MgO	ε_m^θ MgO
3	1.1132×10^{-4}	6.6438×10^{-8}	6.6266×10^{-4}	2.7428×10^{-4}
6	3.5838×10^{-4}	3.48569×10^{-8}	4.24428×10^{-4}	1.59433×10^{-4}
9	2.2229×10^{-6}	2.22825×10^{-10}	3.14409×10^{-5}	2.71522×10^{-5}
12	1.69412×10^{-5}	2.41559×10^{-11}	1.34460×10^{-8}	2.24307×10^{-6}

Table 6. Total squares residual errors for MgO. When $\Pr = 6.3$, $\beta = 0.3$, $\phi_1 = 0.2$, $\phi_2 = 0.4$, $\omega = 0.75$.

	Duwairi[31]	Asifa et al.[10]	Present work
$f'(0)$	0.625	0.62510	0.62512
$-g'(0)$	−1.708	−1.70803	−1.70810
$-\theta'(0)$	−2.264	−0.78555	−0.78557

Table 7. The comparison of the present work with published literature.

- The fluid temperature can be control, with the addition of *Ag-MgO* nanoparticles in the base fluid.
- Magnesium oxide *MgO* compound consists of Mg^{2+} and O^{2-} ions, together bonded by strong ionic bond. Which can be synthesized at 700 °C to 1500 °C and is mostly efficacious for refractory and electrical applications
- The strong bonds between water atom ($H^+ + OH^-$) and silver ions Ag^+ effectively improves the thermophysical properties of water.
- The upward/downward movement of wavy rotating disk positively affects the fluid temperature and velocity.
- The use of hybrid nanoliquid is more efficacious to overcome low energy transmission. Such as, it provides improvement in thermal performance of carrier fluid, which play important role in power generation, hyperthermia, microfabrication, air conditioning and metallurgical field.

Received: 13 August 2020; Accepted: 19 October 2020
Published online: 02 November 2020

References

1. Ma, Y., Mohebbi, R., Rashidi, M. & Yang, Z. Study of nanofluid forced convection heat transfer in a bent channel by means of lattice Boltzmann method. *Phys. Fluids* **30**(3), 032001 (2018).
2. Khoshvaght-Aliabadi, M. Influence of different design parameters and al2o3-water nanofluid flow on heat transfer and flow characteristics of sinusoidal-corrugated channels. *Energy Convers. Manag.* **88**, 96–105 (2014).
3. Rashidi, M., Hosseini, A., Pop, I., Kumar, S. & Freidoonimehr, N. Comparative numerical study of single and two-phase models of nanofluid heat transfer in wavy channel. *Appl. Math. Mech.* **35**(7), 831–848 (2014).
4. Stuart, J. On the effects of uniform suction on the steady flow due to a rotating disk. *Quart. J. Mech. Appl. Math.* **7**(4), 446–457 (1954).
5. Millsaps, K. Heat transfer by laminar flow from a rotating plate. *J. Aeronaut. Sci.* **19**(2), 120–126 (1952).
6. Benton, E. R. On the flow due to a rotating disk. *J. Fluid Mech.* **24**(4), 781–800 (1966).
7. Kuiken, H. The effect of normal blowing on the flow near a rotating disk of infinite extent. *J. Fluid Mech.* **47**(4), 789–798 (1971).
8. Turkyilmazoglu, M. Mhd fluid flow and heat transfer due to a stretching rotating disk. *Int. J. Therm. Sci.* **51**, 195–201 (2012).
9. Tabassum, M. & Mustafa, M. A numerical treatment for partial slip flow and heat transfer of non-newtonian reiner-rivlin fluid due to rotating disk. *Int. J. Heat Mass Transf.* **123**, 979–987 (2018).
10. Tassaddiq, A. *et al.* Heat and mass transfer together with hybrid nanofluid flow over a rotating disk. *AIP Adv.* **10**(5), 055317 (2020).
11. Shuaib, M., Shah, R. A. & Bilal, M. Variable thickness flow over a rotating disk under the influence of variable magnetic field: An application to parametric continuation method. *Adv. Mech. Eng.* **12**(6), 1687814020936385 (2020).
12. S. U. Choi and J. A. Eastman, "Enhancing thermal conductivity of fluids with nanoparticles," tech. rep., Argonne National Lab., IL (United States),1995.
13. Jeon, J., Park, S. & Lee, B. J. Analysis on the performance of a flatplate volumetric solar collector using blended plasmonic nanofluid. *Sol. Energy* **132**, 247–256 (2016).
14. Hussanan, A., Salleh, M. Z., Khan, I. & Shafie, S. Convection heat transfer in micropolar nanofluids with oxide nanoparticles in water, kerosene and engine oil. *J. Mol. Liq.* **229**, 482–488 (2017).
15. Acharya, N. & Mabood, F. On the hydrothermal features of radiative Fe3O4 graphene hybrid nanofluid flow over a slippery bended surface with heat source/sink. *J. Ther. Anal. Calorim.* **2**, 1–17 (2020).
16. Acharya, N. On the flow patterns and thermal behaviour of hybrid nanofluid flow inside a microchannel in presence of radiative solar energy. *J. Ther. Anal. Calorim.* **2**, 1–18 (2019).
17. Motlagh, S. Y. & Soltanipour, H. Natural convection of al2o3-water nanofluid in an inclined cavity using buongiorno's two-phase model. *Int. J. Therm. Sci.* **111**, 310–320 (2017).
18. Acharya, N., Bag, R. & Kundu, P. K. Influence of Hall current on radiative nanofluid flow over a spinning disk: A hybrid approach. *Phys. E* **111**, 103–112 (2019).
19. Akbar, N. S., Raza, M. & Ellahi, R. Influence of induced magnetic field and heat flux with the suspension of carbon nano-tubes for the peristaltic ow in a permeable channel. *J. Magn. Magn. Mater.* **381**, 405415 (2015).
20. Acharya, N., Maity, S. & Kundu, P. K. Influence of inclined magnetic field on the flow of condensed nanomaterial over a slippery surface: The hybrid visualization. *Appl. Nanosci.* **10**(2), 633–647 (2020).
21. Acharya, N., Bag, R. & Kundu, P. K. On the impact of nonlinear thermal radiation on magnetized hybrid condensed nanofluid flow over a permeable texture. *Appl. Nanosci.* **10**(5), 1679–1691 (2020).
22. Liao SJ. The proposed homotopy analysis technique for the solution of nonlinear problems, PhD thesis, Shanghai Jiao Tong University; 1992.
23. Sen, S. *Topology and Geometry for Physicists* (Academic Press Inc., London, 1983).
24. Liao, S. & Tan, Y. A general approach to obtain series solutions of nonlinear differential equations. *Stud. Appl. Math.* **119**(4), 297354 (2007).
25. Hayat, T., Khan, M. & Asghar, S. Magneto hydrodynamic flow of an Oldroyd 6-constant fluid. *Appl. Math Comput.* **155**, 41725 (2004).
26. Sohail, M., Shah, Z., Tassaddiq, A., Kumam, P. & Roy, P. Entropy generation in MHD Casson fluid flow with variable heat conductance and thermal conductivity over non-linear bi-directional stretching surface. *Sci. Rep.* **10**(1), 1–16 (2020).
27. Doh, D. H., Muthtamilselvan, M., Swathene, B. & Ramya, E. Homogeneous and heterogeneous reactions in a nanofluid flow due to a rotating disk of variable thickness using HAM. *Math. Comput. Simul.* **168**, 90–110 (2020).

28. Alreshidi, N. A. *et al.* Brownian motion and thermophoresis effects on MHD three dimensional nanofluid flow with slip conditions and Joule dissipation due to porous rotating disk. *Molecules* **25**(3), 729 (2020).
29. Ma, Y., Mohebbi, R., Rashidi, M. M. & Yang, Z. MHD convective heat transfer of Ag-MgO/water hybrid nanofluid in a channel with active heaters and coolers. *Int. J. Heat Mass Transf.* **137**, 714–726 (2019).
30. Turkyilmazoglu, M. Fluid flow and heat transfer over a rotating and vertically moving disk. *Phys. Fluids* **30**(6), 063605 (2018).
31. Duwairi, H. M. & Damseh, R. A. Magnetohydrodynamic natural convection heat transfer from radiate vertical porous surfaces. *Heat Mass Transfer* **40**(10), 787–792 (2004).
32. Mehmood, A., Usman, M. & Weigand, B. Heat and mass transfer phenomena due to a rotating non-isothermal wavy disk. *Int. J. Heat Mass Transf.* **129**, 96–102 (2019).

Acknowledgements

This work was supported by the Ministry of Education, Malaysia under LRGS Grant with number: LRGS/1/2019/UKM-UKM/5/2.

Author contributions

All authors contributed equally.

Competing interests

The authors declare no competing interests.

Additional information

Correspondence and requests for materials should be addressed to M.A.K.

Reprints and permissions information is available at www.nature.com/reprints.

Publisher's note Springer Nature remains neutral with regard to jurisdictional claims in published maps and institutional affiliations.